Inorg. Chem. **2002**, *41*, 4179–4193

Theoretical Evidence for the Singlet Diradical Character of Square Planar Nickel Complexes Containing Two *o*-Semiquinonato Type Ligands

Vinzenz Bachler,* Gottfried Olbrich, Frank Neese, and Karl Wieghardt*

Max-Planck-Institut für Strahlenchemie, Stiftstrasse 34-36, D-45470 Mülheim an der Ruhr, Germany

Received December 27, 2001

Density functional theory and complete active space self-consistent field computations are applied to elucidate the singlet diradical character of square planar, diamagnetic nickel complexes that contain two bidentate ligands derived from *o*-catecholates, *o*-phenylenediamines, *o*-benzodithiolates, *o*-aminophenolates, and *o*-aminothiophenolates. In the density functional framework, the singlet diradical character is discussed within the broken symmetry formalism. The singlet–triplet energy gaps, the energy gained from symmetry breaking, the spin distribution in the lowest triplet state, and the form of the magnetic orbitals are applied as indicators for the singlet diradical character. Moreover, a new index for the diradical character is proposed that is based on symmetry breaking. All symmetry breaking criteria show that the complexes obtained from *o*-catecholates and *o*-benzodithiolates have the largest and the smallest singlet diradical character, respectively. The singlet diradical character should be intermediate for the complexes derived from *o*-phenylenediamines, *o*-aminophenolates, and *o*-aminothiophenolates. The diradical character of all complexes suggests the presence of Ni(II) central atoms. This is also indicated by the d-populations computed by means of the natural population analysis.

1. Introduction

The electronic structure of square planar, diamagnetic nickel complexes containing two bidentate ligands derived from *o*-catecholates,[1] *o*-phenylenediamines,[2] *o*-benzodithiolates,[3,4] *o*-aminophenolates,[5] and *o*-aminothiophenolates,[6] as shown in Scheme 1, has been a matter of debate since the original discovery of [Ni(*o*-$C_6H_4(NH)_2)_2$] by Feigl and Fürth in 1926[7] and its crystal structure was reported in 1968.[8] The dithiolato analogue [Ni(*o*-$C_6H_4S_2)_2$] has not been obtained in pure form, but Sellmann et al.[9] succeeded in the preparation and crystallographic characterization of [Ni-($^{but}S_2)_2$] where ($^{but}S_2)_2$ represents the ligand 3,5-di-*tert*-butyl-1,2-benzenedithiolate (2−). Similarly, Abakumov et al.[10] reported the complex [Ni($^{but}O_2$)] where ($^{but}O_2)^{2-}$ represents 3,6-di-*tert*-butylcatecholate (2−). We have recently reported the preparation and structures of *trans*-[Ni($^{but}O,N)_2$] and *trans*-[Ni($^{but}S,N)_2$][5a] where ($^{but}O,N)^{2-}$ is *N*-phenyl-3,5-di-*tert*-butyl-*o*-amidophenolate (2−) and ($^{but}S,N)^{2-}$ is 3,5-di-*tert*-butyl-o-amidothiophenolate (2−). The geometrical features of these complexes are displayed in Figure 1.

For all complexes, the experimental ligand geometries imply that the physical oxidation level[11] of these ligands can be described as an open shell, monoanionic π radical (*o*-

* To whom correspondence should be addressed. E-mail: bachler@mpi-muelheim.mpg.de; wieghardt@mpi-muelheim.mpg.de.

(1) (a) Pierpont, C. G.; Lange, C. W. *Prog. Inorg. Chem.* **1994**, *41*, 331.
(2) Mederos, A.; Domiguez, S.; Hernandez-Molina, R.; Sanchiz, J.; Brito, F. *Coord. Chem. Rev.* **1999**, *193*−*195*, 913.
(3) (a) McCleverty, J. A. *Prog. Inorg. Chem.* **1968**, *10*, 49. (b) Schrauzer, G. N. *Transition Met. Chem. (N.Y.)* **1968**, *4*, 299.
(4) Holm, R. H.; Olanov, M. J. *Prog. Inorg. Chem.* **1971**, *14*, 241.
(5) (a) Chaudhuri, P.; Verani, C. N.; Bill, E.; Bothe, E.; Weyhermüller, T.; Wieghardt, K. J. *Am. Chem. Soc.* **2001**, *123*, 2213. (b) Verani, C. N.; Gallert, S.; Bill, E.; Weyhermüller, T.; Wieghardt, K.; Chaudhuri, P. *Chem. Commun.* **1999**, 1747. (c) Chun, H.; Verani, C. N.; Chaudhuri, P.; Bothe, E.; Weyhermüller, T.; Wieghardt, K. *Inorg. Chem.* **2001**, *40*, 4157. (d) Chun, M.; Weyhermüller, T.; Bill, E.; Wieghardt K. *Angew. Chem.* **2001**, *113*, 2552; *Angew. Chem. Int. Ed.* **2001**, *40*, 2489.
(6) Herebian, D.; Bothe, E.; Bill, E.; Weyhermüller, T.; Wieghardt, K. *J. Am. Chem. Soc.* **2001**, *123*, 10012.
(7) Feigl, F.; Fürth, M. *Monatsh. Chem.* **1927**, *48*, 445.
(8) Swartz-Hall, G.; Soderberg, R. H. *Inorg.Chem.* **1968**, *7*, 2300.
(9) Sellmann, D.; Binder, H.; Häussinger, D.; Heinemann, F. W.; Sutter, J. *Inorg. Chim. Acta* **2000**, *300*−*302*, 829.
(10) (a) Abakumov, G. A.; Cherkasov, V. K.; Bubnov, M. P.; Ellert, O. G.; Rakitin, Y. V.; Zakharov, L. N.; Struchkov, Y. T.; Safyanov, Y. N. *Bull. Acad. Sci. USSR, Div. Chem. Sci. (Engl. Transl.)* **1992**, *41*, 1813. (b) Lange, C. W.; Pierpont, C. G. *Inorg. Chim. Acta* **1997**, *263*, 219.
(11) Jörgensen, C. K. In *Oxidation Numbers and Oxidation States*; Springer: Heidelberg, Germany, 1969.

10.1021/ic0113101 CCC: $22.00
Published on Web 07/10/2002

Scheme 1. Definition of Model Complexes **1**−**5** Treated in This Work

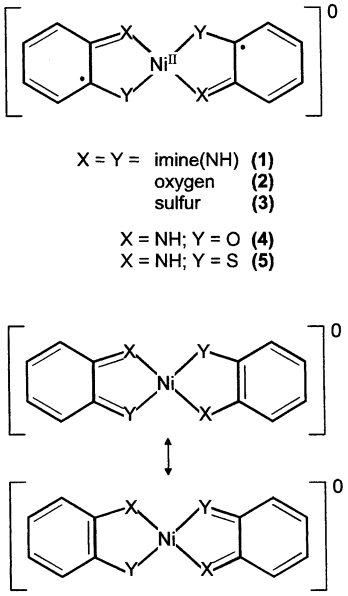

semiquinonato): the C−X and C−Y bond distances are ∼0.04 Å shorter than in their *dianionic*, closed shell aromatic counterparts, and in addition, the C−C bonds of the six-membered rings are not equivalent; they display the quinoid type short−long−short alternating sequence of C−C bonds.

After refuting a higher physical oxidation state than +II (d^8, $S_{Ni} = 0$) for the central nickel atom in the described neutral [NiL_2] complexes,[12] two models for the electronic structures have been seriously, and controversially, discussed in the literature. On one hand, Gray et al.[12] proposed that these species should be considered to be diradicals with a singlet ground state. Holm et al.,[4,13] on the other hand, felt that two resonance structures adequately describe the ground state (Scheme 1).

The two models differ significantly in their molecular orbital description. In a singlet diradical, there are two singly occupied molecular orbitals (SOMOs) of equal energy, and the spins of the two electrons are weakly antiferromagnetically coupled. The closed shell model, however, assumes that a single HOMO is occupied by two electrons with antiparallel spin. Consequently, they occupy the same regions of space in a molecule. A singlet diradical, however, is characterized by two electrons with opposite spins which are separated and weakly antiferromagnetically coupled. To distinguish experimentally between a singlet diradical and a closed shell molecule is a difficult problem because these compounds are diamagnetic even at room temperature. Only for [$Cu^{II}(^{but}O_2)_2$] has an antiferromagnetic coupling between the two *o*-semiquinone ligands of $J = -179$ cm^{-1} been experimentally determined from temperature dependent (70−500 K) magnetic susceptibility measurements.[10] Similarly, for [$Cu^{II}(^{but}O,N)_2$],[5a] an intramolecular antiferromagnetic coupling constant between the two ligand radicals of −400 cm^{-1} has been determined ($H = -2J_{Cu}\cdot J_{rad}$).

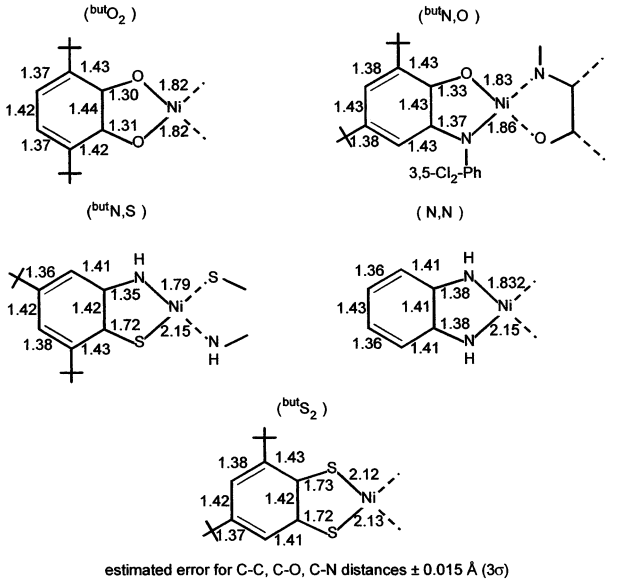

Figure 1. Ring substituted derivatives of model complexes **1**−**5** and their relevant X-ray structure bond lengths. The estimated error for the C−C, C−O, and C−N distances is ±0.015 Å (3σ). A characteristic C−C bond length alternation in the ligands is observed.[10a,5c,6,8,9]

The theoretical first principles treatment of singlet diradicals is a challenging quantum chemical task. Those systems cannot be described by single determinant wave functions which means the application of standard Hartree−Fock (HF) and density functional theory (DFT) methods is insufficient. Accurate post-HF methods are computationally very demanding when applied to systems of the size studied in this work. Therefore, we applied the broken symmetry formalism as introduced by Noodleman[14] that is widely used to compute exchange coupling constants.[15] The broken symmetry formalism is based on the unrestricted Hartree−Fock (UHF) wave function that permits a spatial electron separation in a diradical at the price of point group and spin symmetry breaking.[14] In the symmetry adapted wave function formalism, the singlet diradical state is characterized by the presence of static ("near-degeneracy") correlation and can only be described by a multiconfigurational wave function. In the broken symmetry formalism, however, the static electron correlation is simulated with a symmetry broken single determinant wave function. Using density functional theory (DFT) for a singlet diradical, we might obtain an unrestricted symmetry broken DFT solution that is lower in energy than the restricted solution. This is the basis of the broken symmetry DFT formalism for a computation of antiferromagnetic exchange coupling constants.[16] This reasoning leads

(12) Stiefel, E. I.; Waters, J. H.; Billig, E.; Gray, H. B. *J Am. Chem. Soc.* **1965**, *87*, 3016.
(13) Balch, A. L.; Holm, R. H. *J. Am. Chem. Soc.* **1966**, *88*, 5201.
(14) (a) Noodleman, L. *J. Chem. Phys.* **1981**, *74*. 5737. (b) Noodleman, L.; Davidson, E. R. *Chem. Phys.* **1986**, *109*, 131. (c) Ovchinnikov, A. A.; Labanowski, J. K. *Phys. Rev. A* **1996**, *53*, 3946. (d) Adamo, C.; Barone, V.; Bencini, A.; Totti, F.; Ciofini, I. *Inorg. Chem.* **1999**, *38*, 1996.
(15) (a) Yamaguchi, K.; Tsunekawa, T.; Toyoda, Y.; Fueno, T. *Chem. Phys. Lett.* **1988**, *143*, 371. (b) Hart, J. R.; Rappe, A. K.; Gorun, S. M.; Upton, T. H. *Inorg.Chem.* **1992**, *31*, 5254−5259. (c) Hart, J. R.; Rappe, A. K.; Gorun, S. M.; Upton, T. H. *J. Phys. Chem.* **1992**, *96*, 6264−6269.
(16) For recent work, see for example: Takano, Y.; Shighiro, K.; Onishi, T.; Isobe, H.; Yoshioka, Y.; Yamaguchi, K. *Chem. Phys. Lett* **2001**, *335*, 395. Takano, Y.; Onishi, T.; Kitawa, Y.; Soda, T.; Yoshika, Y.; Yamaguchi, K. *Int. J. Quantum Chem.* **2000**, *80*, 681. Brunhold, T.

immediately to a simple measure for the singlet character of a molecule: *The singlet diradical character of a molecule should be large provided the symmetry broken unrestricted DFT solution for the electronic ground state is much lower in energy than the energy of the restricted singlet ground-state DFT solution.* This criterion has been successfully applied by Houk and co-workers to discuss the singlet diradical character of the transition state of 4 + 2 cycloadditions.[17] Cremer and co-workers used this DFT criteria to investigate the singlet diradical character of the transition state of the Bergmann reaction.[18] Thus, a singlet diradical is characterized by the presence of an instability of the restricted DFT solution.

We investigate in this work the electronic structure of Ni complexes **1**−**5** by means of DFT and the complete active space self-consistent field (CASSCF) method. A new measure for the diradical character is presented that is derived within the broken symmetry wave function formalism. The computational results indicate that, with the exception of the sulfur complex **3**, all complexes have a significant diradical character that supports the description of the complexes given at the top of Scheme 1.

2. Computational Details

All DFT calculations were performed by means of the Gaussian98 suite of ab initio programs.[19,20] For the nickel atom, the basis set developed by Dolg et al.[21] has been employed as referenced by the Gaussian keyword SDD. This basis set describes the Ne core of the Ni atom by a relativistic pseudopotential. Thus, a small core[22] is used for the Ni atom. The remaining s, p, and d valence electrons are explicitly used to describe the bonding in the Ni complexes. The s atomic orbitals (AOs) are simulated by 8 primitive Gaussians that are grouped according to the contraction scheme (8s/311111).[21] The p AOs are simulated by the contraction scheme (7p/22111).[21] A basis set of triple-ζ quality, namely (6d/411),[21] is used for the important d AOs. Moreover, this Ni basis set comprises also one set of f Gaussians.[21] Thus, a basis set of rather large flexibility has been employed to describe the Ni atoms in the Ni−N, Ni−O, and Ni−S bonds. For the remaining atoms, the 6-31G* all valence basis sets[23a] were used that comprise d polarization functions for C, N, O, and S atoms.[23b] We applied these basis sets in the framework of the restricted B3P86 DFT scheme to compute the geometries of **1**−**5**. The nonhybrid BP86 DFT procedure combined with our selected basis sets, but supplemented by p polarization functions on the hydrogens, produced previously excellent geometries and vibrational frequencies for transition metal carbonyls as shown by Jonas and Thiel.[24] Thus, we used the same correlation functional as Jonas and Thiel[24] but the hybrid exchange functional. This combination of functionals also produced in the past good geometries and vibrational frequencies for $V(CO)_6^-$ and $Cr(CO)_6$.[25] We imposed D_{2h} symmetry in the computations for the complexes **1**−**3** but C_{2h} symmetry for **4** and **5**.

The approximate restricted DFT solution for a singlet diradical should be unstable, and a symmetry broken DFT solution of lower energy should exist. For **1**−**5**, such solutions were detected by testing the stability of the restricted DFT solution. This was performed by means of the stability analysis of Seeger and Pople[26] as referenced by the Gaussian keyword STABLE=OPT.[19] This keyword coaxes G98 to perform the stability analysis.[19] If a restricted DFT solution is found to be unstable, the modification of STABLE by OPT induces G98 to find automatically an unrestricted and symmetry broken DFT solution of lower energy.[19] Those symmetry broken solutions were in addition verified by starting from the restricted solution and an application of the MIX option.[19] This option produces symmetry broken guess orbitals by forming the plus and minus linear combination of the symmetry adapted restricted frontier guess orbitals. By using this symmetry broken guess orbitals, we obtained symmetry broken DFT solutions. Their energies were identical to the energies of the symmetry broken solutions obtained by means of the stability analysis. The presence of a symmetry broken solution is also indicated by an S^2 expectation value that is different from zero (Table 4). The stability analysis was performed with the same basis sets as applied for the geometry optimizations, but we employed the B3LYP DFT scheme[27] which is known to produce rather accurate exchange coupling constants.[28] To obtain accurate DFT solutions, the tight SCF convergence criteria[19] and the ultrafine integration grid[19] were employed. The natural population analysis (NPA) developed by Weinhold and co-workers[29] was carried out with the natural bond orbital (NBO)

C.; Solomon, E. I. *J. Am. Chem. Soc.* **1999**, *121*, 8277. Cano, J.; Ruiz, E.; Alemany, P.; Lloret, F.; Alvarez, S. *J. Chem. Soc., Dalton Trans.* **1999**, 1669−1676. Demachy, I.; Jean, Y.; Lledos, A. *Chem. Phys. Lett.* **1999**, *303*, 621. Caneschi, A.; Fabrizi de Biani, F.; Kloo, L.; Zanello, P. *Int. J. Quantum Chem.* **1999**, *72*, 61−71. Rodrigues, J. H.; Wheeler, D. E.; McCusker, J. K. *J. Am. Chem. Soc.* **1998**, *120*, 12051−12068. Lledos, A.; Jean, Y. *Chem. Phys. Lett.* **1998**, *287*, 243−249. Cano, J.; Alemany, P.; Alvarez, S.; Verdaguer, M.; Ruiz, E. *Chem.−Eur. J.* **1998**, *4*, 476. Kuramochi, H.; Noodleman, L.; Case, D. A. *J. Am. Chem. Soc.* **1997**, *119*, 11442−11451. Bencini, A.; Totti, F.; Daul, C. A.; Docio, K.; Fantucci, P.; Barone, V. *Inorg.Chem.* **1997**, *36*, 5022.

(17) Goldstein, E.; Beno, B.; Houk, K. N. *J. Am. Chem Soc* **1996**, *118*, 6036−6043.

(18) Gräfenstein, J.; Hjerpe, A. M.; Kraka, E.; Cremer, D. *J. Phys. Chem. A* **2000**, *104*, 1748

(19) Frisch, M. J.; Trucks, G. W.; Schlegel, H. B.; Scuseria, G. E.; Robb, M. A.; Cheeseman, J. R.; Zakrzewski, V. G.; Montgomery, J. A., Jr.; Stratmann, R. E.; Burant, J. C.; Dapprich, S.; Millam, J. M.; Daniels, A. D.; Kudin, K. N.; Strain, M. C.; Farkas, O.; Tomasi, J.; Barone, V.; Cossi, M.; Cammi, R.; Mennucci, B.; Pomelli, C.; Adamo, C.; Clifford, S.; Ochterski, J.; Petersson, G. A.; Ayala, P. Y.; Cui, Q.; Morokuma, K.; Malick, D. K.; Rabuck, A. D.; Raghavachari, K.; Foresman, J. B.; Cioslowski, J.; Ortiz, J. V.; Stefanov, B. B.; Liu, G.; Liashenko, A.; Piskorz, P.; Komaromi, I.; Gomperts, R.; Martin, R. L.; Fox, D. J.; Keith, T.; Al-Laham, M. A.; Peng, C. Y.; Nanayakkara, A.; Gonzalez, C.; Challacombe, M.; Gill, P. M. W.; Johnson, B. G.; Chen, W.; Wong, M. W.; Andres, J. L.; Head-Gordon, M.; Replogle, E. S.; Pople, J. A. *Gaussian 98*, revision A.5; Gaussian, Inc.: Pittsburgh, PA, 1998.

(20) We thank R. Trinoga for the implementation of G98 at the Origin 2000 and Es40 computers.

(21) Dolg, M.; Wedig, U.; Stoll, H.; Preuss, H. *J. Chem. Phys.* **1987**, *86*, 866.

(22) See for example: Frenking, G.; Antes, I.; Boehme, M.; Dapprich, S.; Ehlers, A. W.; Jonas, V.; Neuhaus, A.; Otto, M.; Stegman, R.; Veldkamp, A.; Vyboishikov, S. F. *Reviews in Computational Chemistry*; Lipkowitz, K.-B., Boyd, D. B., Eds.; VCH, New York, 1996; vol. 8, p 63 ff, in particular, p 72, Point 2.

(23) (a) Hehre, W. J.; Ditchfield, R.; Pople, J. A. *J. Chem Phys.* **1972**, *56*, 2257. (b) Hariharan, P. C.; Pople, J. A. *Theor. Chim. Acta* **1973**, *28*, 213.

(24) Jonas, V.; Thiel, W. *J. Chem. Phys.* **1995**, *102*, 8474. Jonas, V.; Thiel, W. *J. Chem. Phys.* **1996**, *105*, 3636.

(25) Spears, K. G. *J. Phys. Chem. A* **1997**, *101*, 6273.

(26) Seeger, R.; Pople, J. A. *J. Chem. Phys.* **1977**, *66*, 3045.

(27) Becke, A. D. *J. Chem. Phys.* **1993**, *98*, 5648. Lee, C.; Yang, W.; Parr, R. G. *Phys. Rev. B* **1988**, *37*, 785. Miehlich, B.; Savin, A.; Stoll, H.; Preuss, H. *Chem. Phys. Lett.* **1989**, *157*, 200.

(28) See for example: Ruiz, E.; Cano, J.; Alvarez, S.; Alemany, P. *J. Comput. Chem.* **1999**, *20*, 1391 in particular Tables I and III.

(29) Reed, A. E.; Weinhold, F. *J. Chem. Phys.* **1983**, *78*, 4066. Reed, A. E.; Weinstock, R. B.; Weinhold, F. *J. Chem. Phys.* **1985**, *83*, 735. For a review see: Reed, A. E.; Curtiss, L. A.; Weinhold, F. *Chem. Rev.* **1988**, *88*, 899.

package of Gaussian 98.[19] Moreover, we performed CASSCF calculations with two "magnetic" electrons in eight orbitals. They were selected on the basis of the occupation numbers of the natural orbitals derived from the symmetry broken UHF electron densities.

3. A Simple Index for the Diradical Character

In the subsequent paragraphs, we will apply diradical criteria within the symmetry breaking formalism[14,16] which is based on the UHF wave function.[14] Noodleman and Davidson showed that all important perturbational contributions that determine the exchange coupling constants J are contained in the UHF wave function.[14b] Salem and Rowland showed in their classic paper[30] that for diradicals correlated wave functions are mandatory. In particular, the diradical wave function must account for a homolytic separation of the two electrons of a spin coupled electron pair. In this paragraph, we illustrate the appropriateness of the UHF wave function and of the simplest restricted correlated wave function to describe diradicals. This treatment leads to new indices which are a measure for the diradical character of molecules.

Let us assume an electronic system can be reduced to the problem of two electrons in two magnetic orbitals χ_A and χ_B localized on the sites A and B, respectively. We can form the bonding and antibonding MOs ϕ_i and ϕ_j,[30] respectively,

$$\phi_1 = (\chi_A + \chi_B)/\sqrt{2 + 2S_{AB}} \tag{1a}$$

$$\phi_2 = (\chi_A - \chi_B)/\sqrt{2 - 2S_{AB}} \tag{1b}$$

and S_{AB} is the overlap integral between χ_A and χ_B. Let us now consider a system A−B with a weak electronic intersite interaction. An UHF computation would produce two occupied MOs a and b which are not symmetry adapted in the point group of the molecule and are preferentially localized on A and B, respectively. Thus, the resulting UHF Slater determinant

$$\Psi_{UHF}(a\bar{b}) \equiv \frac{1}{\sqrt{2}}\begin{vmatrix} a(1) & a(2) \\ \bar{b}(1) & \bar{b}(2) \end{vmatrix} \tag{2}$$

is space and spin symmetry broken, and a and b are the magnetic orbitals of the model system A−B. We now assume that ϕ_1 and ϕ_2 are the bonding and antibonding MOs obtained from a restricted Hartree−Fock (RHF) computation. We can expand the MOs a and b into the set of ϕ_1 and ϕ_2 as done by Szabo and Ostlund.[31]

$$a = \cos\vartheta\phi_1 + \sin\vartheta\phi_2 \tag{3a}$$

$$b = \cos\vartheta\phi_1 - \sin\vartheta\phi_2 \tag{3b}$$

This transformation linearly combines the symmetry adapted MOs ϕ_1 and ϕ_2, and the combination depends on the angle θ.[31] The transformation in eq 3 is not a rotation in the mathematical sense, but we will refer to θ as the "rotational angle". If ϕ_1 and ϕ_2 are the natural orbitals, obtained within a restricted CI procedure, eq 3 provides the formulas of Yamaguchi et al. for the determination of the magnetic orbitals.[32] The authors, however, did not determine the rotational angle θ, but they used the reasonable value of $\theta = 45°$.[33] By means of eq 3, we expand $\Psi_{UHF}(a\bar{b})$ into the form

$$\Psi_{UHF}(a\bar{b}) = \frac{1}{\sqrt{2}}[\cos^2\vartheta\Phi(1\bar{1}) + \sin\vartheta\cos\vartheta(\Phi(2\bar{1}) - \Phi(1\bar{2})) - \sin^2\vartheta\Phi(2\bar{2})] \tag{4}$$

The symbols Φ designate two-by-two Slater determinants (without normalization factor) that contain the restricted MOs ϕ_1 and ϕ_2. $\Phi(1\bar{1})$ is the closed shell ground state Slater determinant with a doubly occupied MO ϕ_1. The determinant $\Phi(2\bar{2})$ is also closed shell but represents a double excitation into the antibonding MO ϕ_2. The two determinants $\Phi(2\bar{1})$ and $\Phi(1\bar{2})$ describe single excitations. The closed shell determinants $\Phi(1\bar{1})$ and $\Phi(2\bar{2})$ are eigenfunctions of the total spin operator S^2. One can show that the difference function $\Phi(2\bar{1}) - \Phi(1\bar{2})$ in eq 4 is a spin pure triplet wave function with $M_s = 0$. Thus, the UHF wave function $\Psi_{UHF}(a\bar{b})$ for our model diradical is not spin pure[31] but a linear combination of singlet and triplet components. We can use eq 1 to expand the MO Slater determinants in eq 4 into Slater determinants composed of the AOs χ_A and χ_B and we obtain

$$\Phi(1\bar{1}) = \frac{1}{2 + 2S_{AB}}[\Phi(A\bar{A}) + \Phi(A\bar{B}) + \Phi(B\bar{A}) + \Phi(B\bar{B})] \tag{5a}$$

$$\Phi(1\bar{2}) = \frac{1}{(2 + 2S_{AB})(2 - 2S_{AB})}[\Phi(A\bar{A}) - \Phi(A\bar{B}) + \Phi(B\bar{A}) - \Phi(B\bar{B})] \tag{5b}$$

$$\Phi(2\bar{1}) = \frac{1}{(2 - 2S_{AB})(2 + 2S_{AB})}[\Phi(A\bar{A}) + \Phi(A\bar{B}) - \Phi(B\bar{A}) - \Phi(B\bar{B})] \tag{5c}$$

$$\Phi(2\bar{2}) = \frac{1}{2 - 2S_{AB}}[\Phi(A\bar{A}) - \Phi(A\bar{B}) - \Phi(B\bar{A}) + \Phi(B\bar{B})] \tag{5d}$$

The symbols $\Phi(A\bar{A})$, $\Phi(A\bar{B})$, $\Phi(B\bar{A})$, and $\Phi(B\bar{B})$ designate Slater determinants composed of the AOs χ_A and χ_B that are localized at sites A and B, respectively. By substituting eq 5a−d into 4, we realize that $\Phi(A\bar{A})$, $\Phi(B\bar{B})$ and $\Phi(A\bar{B})$, $\Phi(B\bar{A})$ are the ionic and covalent contributions of $\Psi_{UHF}(a\bar{b})$. Their relative weighting is a function of the angle θ as indicated by eq 4. This angle is determined by the variational principle[34] that minimizes the electronic energy at a fixed intersite distance. To discuss the ratio between the ionic and

(30) Salem, L.; Rowland, C. *Angew. Chem.* **1972**, *84*, 86; *Angew. Chem. Int. Ed.* **1972**, *11*, 92.
(31) Szabo, A.; Ostlund, N. S. *Modern Quantum Chemistry*; McGraw-Hill, New York, 1989; in particular, chapter 3.8.7, p 221.
(32) See for example: Yamaguchi, K.; Okamura, M.; Takada, K.; Yamanaka, S. *Int. J. Quantum Chem., Quantum Chem. Symp.* **1993**, *27*, 501 in particular, eqs 2a and 2b.
(33) See ref 32, in particular, the lines below eqs 2a and 2b.
(34) See for example: McWeeny, R. *Methods of Molecular Quantum Mechanics*; Academic Press: London, 1996; in particular, section 2.4, p 40.

the covalent contributions in $\Psi_{UHF}(a\bar{b})$, we propose a simple method for the determination of θ. A symmetry broken $\Psi_{UHF}(a\bar{b})$ is characterized by an expectation value over the total spin operator S^2. A simple relationship between the spin expectation value $\langle\Psi_{UHF}(a\bar{b})|S^2|\Psi_{UHF}(a\bar{b})\rangle$ and $\cos^2\theta$ exists, namely

$$\cos^2\vartheta = \frac{1+\sqrt{1-\langle\Psi_{UHF}(a\bar{b})|S^2|\Psi_{UHF}(a\bar{b})\rangle}}{2} \qquad (6)$$

that leads to a discussion of the diradical properties of $\Psi_{UHF}(a\bar{b})$ as a function of the spin expectation value. If $\langle\Psi_{UHF}(a\bar{b})|S^2|\Psi_{UHF}(a\bar{b})\rangle$ is zero, eq 6 produces a $\cos 2\theta$ value of 1. If we substitute this value into eq 4 and use eq 5a, $\Psi_{UHF}(a\bar{b})$ appears in the form

$$\Psi_{UHF}(a\bar{b}) = \frac{1}{\sqrt{2}(2+2S_{AB})}[\Phi(A\bar{A}) + \Phi(A\bar{B}) + \Phi(B\bar{A}) + \Phi(B\bar{B})] \quad (7)$$

Thus, $\Psi_{UHF}(a\bar{b})$ is identical to the restricted closed shell singlet solution $\Phi(1\bar{1})$, and ionic and covalent AO Slater determinants appear with the same weight. If $\langle\Psi_{UHF}(a\bar{b})|S^2|\Psi_{UHF}(a\bar{b})\rangle$ is equal to 1, eq 6 produces a $\cos^2\theta$ value of $^1/_2$ that corresponds to a θ value of 45°. We realize that for such a θ all four Slater determinants in eq 4 appear with the same coefficients. Substitution of eq 5a−d into eq 4 leads to a complete cancellation of the ionic contributions, and we obtain

$$\Psi_{UHF}(a\bar{b}) = \frac{2}{\sqrt{2}(2+2S_{AB})}\Phi(A\bar{B}) \qquad (8)$$

If S_{AB} is very small, $\Psi_{UHF}(a\bar{b})$ has the simple form

$$\Psi_{UHF}(a\bar{b}) = \frac{1}{\sqrt{2}}\Phi(A\bar{B}) \qquad (9)$$

Therefore, $\Psi_{UHF}(a\bar{b})$ is solely determined by a covalent contribution. Salem and Rowland have shown that this is characteristic for a diradical wave function.[35] Thus, $\Psi_{UHF}(a\bar{b})$ is a diradical wave function provided $\langle\Psi_{UHF}(a\bar{b})|S^2|\Psi_{UHF}(a\bar{b})\rangle$ is equal to 1. This accords with the notion that in the weak interaction limit the singlet and triplet states have the same energy and $\Psi_{UHF}(a\bar{b})$ is an equal mixture of singlet and triplet components.

This analysis leads to a simple measure for the diradical character in a system where two electrons are distributed in two orbitals. If $\cos^2\theta$ is equal to $^1/_2$, the electronic system has a diradical character of 100%. If, on the other hand, $\cos^2\theta$ is equal to 1, the electronic system is a restricted closed shell molecule where covalent and ionic parts appear with equal weights.[36] We attribute to such a system a diradical character of 0%. Equation 6 and this reasoning lead to an index n_{rad} for the diradical character:

$$n_{rad} \equiv 200\sin^2\theta = 100(1-\sqrt{1-\langle\Psi_{UHF}(a\bar{b})|S^2|\Psi_{UHF}(a\bar{b})\rangle}) \quad (10)$$

In essence, it is $\sin^2\theta$ which is the configuration interaction coefficient for the doubly excited configuration (see eq 4). Thus, the diradical character of a molecule is 100% and 0% provided $\langle\Psi_{UHF}(a\bar{b})|S^2|\Psi_{UHF}(a\bar{b})\rangle$ is 1 and zero, respectively. The index n_{rad} is closely related to the index defined long ago by Yamaguchi.[37] His index is the square of the configuration interaction coefficient for the doubly excited configuration and was determined by means of the overlap of the corresponding magnetic orbitals.[37] We, however, compute the coefficient from the calculated spin expectation value of the symmetry broken wave function for *all* electrons.

The simplest correlated two-electron wave function Ψ_0 that describes a singlet ground state of a diradical is given by

$$\Psi_0 = c_0\,\Phi(1,\bar{1}) + c_d\,\Phi(2,\bar{2}) \qquad (11)$$

Here, c_0 and c_d are the configuration interaction (CI) coefficients of the two-by-two CI problem. By substituting eq 5a,d into eq 11, we observe that in Ψ_0 a cancellation of ionic wave functions $\Phi(A\bar{A})$ and $\Phi(B\bar{B})$ occurs provided c_0 and c_d are equal and of opposite sign. One can show, at least for the 2 × 2 eigenvalue problem, that c_0 and c_d have opposite sign. If $|c_0| = |c_d|$ holds, and the intersite overlap S_{AB} can be neglected, Ψ_0 describes a purely covalent singlet diradical.

$$\Psi_0(\text{rad}) = \frac{1}{\sqrt{2}}[\Phi(A\bar{B}) + \Phi(B\bar{A})] \qquad (12)$$

Ψ_0(rad) is a singlet eigenfunction and has previously been obtained by Salem and Rowland to describe singlet diradicals.[38] If $|c_d|$ in eq 11 is $1/\sqrt{2}$, the compound should have a singlet diradical character of 100%. Contrary, a c_d value of zero indicates a closed shell molecule in the restricted HF approximation. Again, we attribute to such a closed shell molecule a singlet diradical character of zero. This reasoning leads to a simple index for the singlet diradical character, namely

$$n_{rad} = 100|c_d|\sqrt{2} \qquad (13)$$

In section 5 and 6, we apply eqs 10 and 13 to evaluate the diradical characters of target complexes **1**−**5**.

4. Results

4.1. Computed Geometries. The computed bond lengths for **1**−**5** are shown in Figure 2. The optimized bond lengths for complex **1** agree reasonably well with those obtained from an X-ray structure analysis.[8] For most bond lengths, a deviation from experiment in the range 0.01−0.03 Å is computed. This might result from the rather low resolution of the formerly applied experimental technique.[8] Slightly larger deviations are found for the N−C bonds, and the

(35) See ref 30, in particular, eq 6 on p 91.
(36) Mulliken, R. S. *Phys. Rev.* **1932**, *41*, 49. Slater, J. C. *J. Chem. Phys.* **1965**, 43, S11. For butadiene and benzene see Table 2 in: Hiberty, P. C.; Ohanessian, G. *Int. J. Quantum Chem.* **1985**, *27*, 245.
(37) Yamaguchi, K. *Chem. Phys. Lett.* **1975**, *33*, 330.
(38) See ref 30, eq 6.

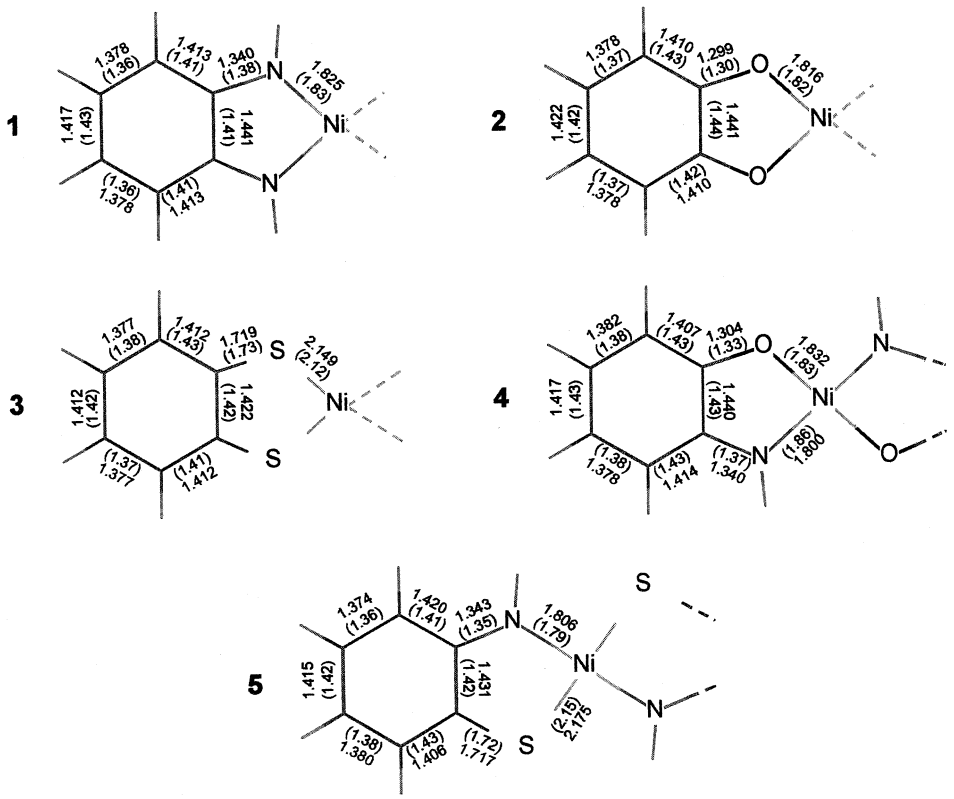

Figure 2. Comparison of computed and experimental bond lengths. The experimental values are given in brackets. The computed and experimental bond lengths deviate at most 0.03 Å.

Ni−N bond lengths are well reproduced. The good agreement with experiment is further support for the known fact that DFT reproduces well the geometries of transition metal complexes.[39] In accord with experiment, a significant bond length alternation in the ligands is computed. All four C−N bond lengths are about 1.34 Å. The average of several experimental parafinic C−N bond lengths is 1.472 Å.[40] Therefore, the four N−C bonds in **1** should have a significant double bond character. The computed and experimental[10a] bond lengths for **2** deviate only about 0.02 Å. This holds true also for the Ni−O bond lengths. As for **1**, a pronounced C−C bond length alternation in the ligands is computed for complex **2**. The agreement between experimental[41] and computed bond lengths is also satisfactory for **3** but only when d polarization functions at the sulfur atoms were provided. In particular, the C−C bond length alternation in the ligands is reproduced (Figure 2). Lauterbach and Fabian have previously computed the geometry of **3** by means of the B3LYP DFT method.[42] Their calculated S−Ni and C−S distances of 2.173 and 1.728 Å, respectively, agree well with our values of 2.149 and 1.719 Å. The computed bond lengths for **4** and **5** (Figure 2) accord with the bond lengths obtained from the high-resolution X-ray structure analysis.[5a] To sum up, the experimental geometries of **1**−**5** are well reproduced by the DFT computations, and the observed carbon−carbon bond length alternation in the ligands is satisfactorily reproduced.

We have obtained agreement with experiment by performing restricted closed shell DFT computations for **1**−**5**. Thus, we tacitly neglected a diradical character in the geometry optimizations. We also performed a full geometry optimization of the B3P86 symmetry broken state of complex **2**. Such an electronic state is fictitious and without a rigorous physical meaning. For molecules exhibiting a weak antiferromagnetic coupling, however, symmetry broken DFT solutions can lead to geometries that are in better agreement with experiment than the geometries based on space and spin symmetry adapted closed shell DFT solutions.[43] The calculated geometry for **2** was found to be almost identical to the geometry obtained within the restricted DFT scheme. Only the Ni−O bond lengths are slightly longer than the experimental bond lengths. The agreement with the experimental geometry, achieved without consideration of the diradicaloid character, shows that geometrical features alone are insufficient to indicate a singlet diradical character. In the following sections, we pursue alternative ways to determine the singlet diradical character.

4.2. Charge Distributions in the Symmetry Broken States. A diradical character of **1**−**5** is only compatible with the presence of a Ni(II) central atom as indicated by an Ard[8]

(39) For reviews see for example: (a) Ziegler, T. *Chem. Rev.* **1991**, *91*, 651. (b) Delley, B. In *Density Functional Theory, A Tool for Chemistry*; Seminario, J. M., Politzer, P., Eds.; Elsevier: Amsterdam 1994. (c) Koch, W.; Holthausen, M. C. *A Chemist's Guide to Density Functional Theory*; Verlag Chemie: Weinheim, Germany 2000.

(40) *Tables of Interatomic Distances and Configuration in Molecules and Ions*; The Chemical Society: London, 1958, S16.

(41) See ref 9, in particular, Table 2.

(42) Lauterbach, C.; Fabian, J. *Eur. J. Inorg. Chem.* **1999**, 1995 in particular, Table 1.

(43) Lovell, T.; McGrady, J. E.; Stranger, R.; Macgregor, S. A. *Inorg. Chem.* **1996**, *35*, 3079−3080.

Table 1. Electron Populations of the 3d, 4s, and 4p Shells of the Central Ni Atoms for **1**−**5**[a]

complex	3d	4s	4p
N(**1**)	8.60	0.38	0.04
O(**2**)	8.49	0.36	0.03
S(**3**)	8.93	0.48	0.05
N, O(**4**)	8.54	0.37	0.03
N, S(**5**)	8.74	0.43	0.04

[a] They were obtained by means of the natural populations analysis (NPA).[29] The d populations indicate a Ni(II) oxidation state of the central Ni atoms. The relative values of the 4s and 4p population should be considered with caution (see text).

electron configuration with $S_{Ni} = 0$. To determine this electron configuration, a natural population analysis (NPA)[29] for **1**−**2** and **4**−**5** was performed on the basis of the symmetry broken DFT densities. For **3**, we employed the restricted DFT density. Maseras and Morokuma have shown that the total NPA charges of a transition metal in a complex may depend critically on the inclusion or the exclusion of the 4p orbitals into the set of strongly occupied valence orbitals.[44] In particular, the relative populations of the 4s and 4p orbitals are affected.[44] The population of 3d orbitals, however, seems to be rather unaffected.[45] The NPA results for the central Ni atoms are compiled in Table 1. As expected, the valence electrons prefer the 3d AOs. Much smaller electron density is located in the 4s−4p shells, and their relative occupation should be considered with caution.[44] About 8.6 electrons are located in the 3d orbitals of **1**. This value is slightly lower than 8.9, a value computed by Weber et al. with the Xα method.[46] In view of the different approaches used, we feel that the agreement is reasonable. For **3**, we computed a value of 8.93 which indicates that in **3** also a +II oxidation state of the central Ni atom is present. The charge excess over the formal d^8 configuration of low-spin Ni(II) arises from a charge transfer from the ligands to the central Ni atom that leads to weak covalent bonding. Nevertheless, the computed populations for **1**−**5** are typical for a +II oxidation state of the central nickel ion.

4.3. Spin Density Distribution in the Triplet State. Before studying the antiferromagnetic coupling in the target complexes, it is instructive to inspect the spin distribution in the corresponding triplet states. For this purpose, we assume that the weakly spin coupled electrons in a singlet diradical and the corresponding electrons in a triplet radical are located at the same position of a molecule. Only a simple spin inversion converts the singlet into the triplet radical.

In Figure 3, we have represented the Mulliken spin densities of the lowest triplet state of model complexes **1**−**5**. They are the basis of Table 2 where the total spin densities located at all ring carbon atoms are represented.[47] Moreover, the spin densities at the atoms bonded to the nickel atom and at the nickel atoms are given. The sums of the ring carbon spin densities increase in the sequence **3** < **5** < **1** < **4** < **2**. This indicates the ordering of spin density delocalization which should also hold for the corresponding singlet diradicals. If resonance stabilization favors the singlet diradical character, it should increase in the sequence **3** < **5** < **1** < **4** < **2**. The large ring delocalization in **2** leads to a spin density at the oxygen atoms which is significantly smaller than the spin densities at the corresponding hetero-

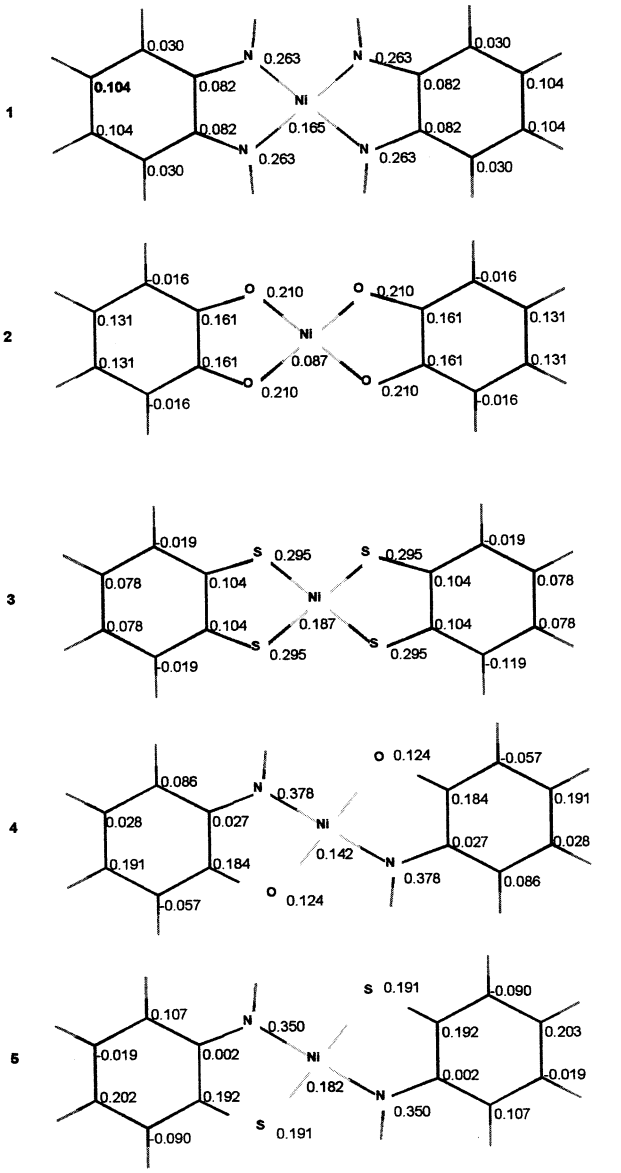

Figure 3. Computed triplet Mulliken spin densities for **1**−**5**. The largest ring delocalization of the spin density occurs in oxygen complex **2**. The smallest ring delocalization of the spin density occurs in sulfur complex **3** (see text).

Table 2. Triplet Spin Densities for **1**−**5** Located at the Ring Carbons, the Atoms Bonded to the Ni Atoms, and the Ni Atom Itself[a]

complex	ring	(N) (O) (S)	Ni
N(**1**)	0.846	1.052	0.165
O(**2**)	1.104	0.840	0.087
S(**3**)	0.652	1.180	0.187
N,O(**4**)	0.918	1.004	0.142
N, S(**5**)	0.788	1.082	0.182

[a] The largest delocalization of the spin density occurs in the triplet state of **2**. The resonance stabilization of the singlet diradical **2** should be most pronounced (see text).

(44) Maseras, F.; Morokuma, K. *Chem. Phys. Lett.* **1992**, *195*, 500. We thank one referee for pointing out the importance of this reference.
(45) See ref 44, Table 1.
(46) Weber, J.; Daul, C.; Von Zelewsky, A.; Goursot, A.; Penigault, E. *Chem. Phys. Lett.* **1982**, *88*, 78.
(47) At the hydrogen atoms negative spin densities are computed.

atoms in **1**, **3**, **4**, and **5**. The large spin density of 1.180 at the sulfur atoms of **3** and the smallest spin density in the ligand rings supports the notion that in the singlet diradical of **3** the unpaired electrons are mainly localized at the sulfur atoms. Because of their proximity, a large antiferromagnetic coupling arises which leads to a small diradical character of **3**.

4.4. Magnetic Orbitals and Singlet Diradical Character. The symmetry broken DFT solutions for a singlet diradical are characterized by Kohn−Sham (KS) spin-orbitals whose space parts are different for the α and β electrons. If an α and a β electron are weakly antiferromagnetically coupled, their orbitals are called the magnetic orbitals.[48] This often implies that the average distance between the two weakly coupled electrons is rather large and the magnetic orbitals are localized in different regions of the molecule.[49] In the case of a strong antiferromagnetic coupling, the two electrons can approach each other, and their orbitals should be similar in shape. This reasoning leads to a qualitative recipe to single out the magnetic orbitals from the sets of the occupied α and β KS orbitals.[50a]

Consider one occupied α KS orbital. If we can find an occupied β KS orbital similar in shape to the α orbital, the two orbitals are occupied by electrons that are strongly antiferromagnetically coupled. *If we cannot find an occupied β orbital that matches the shape of the α orbital, the α KS orbital is a magnetic orbital.*[51] The qualitative procedure is illustrated in Figure 4 for **1**. Almost all α orbitals match with a β orbital. The only exceptions are the highest occupied α and β orbitals that match with unoccupied orbitals (not shown). Therefore, the highest occupied α and β orbitals are the magnetic orbitals for model complex **1**. We observe that almost *all* KS orbitals are not symmetry adapted in the D_{2h} point group of **1** (Figure 4). This indicates that spin polarization influences the distribution of *all* mobile π electrons in the symmetry broken state.

Another way to identify the magnetic orbitals is to use the corresponding orbital transformation of Amos and Hall.[52] In this method, the spin-up and spin-down orbitals are each subjected to a unitary transformation such that each spin-up orbital overlaps with only one spin-down orbital. Orbitals that only weakly overlap are called the "magnetic orbitals" of the system. For complexes **1**−**5**, this transformation results in spin-up/spin-down pairs that have an overlap of >0.99. The only exception is one pair that is made up by the spatially nonorthogonal magnetic orbitals. Their forms turned out to be almost identical to the shapes of the magnetic orbitals singled out by the described qualitative inspection technique. The magnetic orbitals of **1**, **2**, **4**, and **5** are shown in Figure 5 where contour surface values of 0.05 are plotted.[53] All magnetic orbitals for the α spin electron are mainly localized at one ligand. The magnetic orbitals for the β spin electron, however, are situated at the other ligand. They closely correspond to the π HOMOs of the free semiquinonate ligands. The d orbitals of the central nickel atoms contribute only marginally to the magnetic orbitals. This indicates a closed shell character of the Ni atoms in **1**, **2**, **4**, and **5**. This finding is compatible with presence of a Ni(II) valence state which was indicated by the NPA electron populations in the Ni d shell (section 4.2). The sulfur complex, **3**, does not spontaneously break symmetry. In Figure 5, we have depicted the highest doubly occupied KS orbital of **3** which is, of course, symmetry adapted in the D_{2h} point group of **3**.

4.5. Computed Singlet−Triplet Energy Gaps. In a singlet diradical, two electrons with opposite spin are weakly antiferromagnetically coupled. Therefore, only a small amount of energy is needed to invert one spin, and a small singlet−triplet energy gap is characteristic for a singlet diradical.[54] The symmetry broken DFT formalism[16] has been extensively applied in the past to compute the exchange coupling constants that determine the singlet−triplet energy gaps. In this section, we employ this computational scheme to model complexes **1**−**5**. We calculated the singlet−triplet energy gap as

$$E_s - E_t = E(b) - E_u(T_1) \qquad (14)$$

which is the difference between the energy of the symmetry broken state and the UHF energy of the high spin triplet state, respectively.[55] This formula holds in the wave function formalism for the strong coupling case[50a] that is the strong delocalization limit. Consequently, the use of eq 14 to describe weakly spin coupled electrons as in diradicals is probably unjustified. Nevertheless, the strong coupling formula produces *rather* accurate exchange coupling constants in the symmetry broken DFT procedure,[55] even when the electron spins are only weakly coupled. This fortunate agreement with experiment seems to arise from a cancellation of errors as pointed out by Caballol et al.[56] The symmetry breaking DFT formalism yields singlet−triplet gaps that are too large by about a factor of 2.[56] This factor vanishes if one assumes (illegitimately) the strong delocalization limit.[56] The only justification might be the larger delocalization of the Kohn−Sham orbitals as compared to the UHF MOs.[56] Caballol et al. suggest a general formula for the singlet-triple gap that holds for the whole range of spin coupling strengths.[56]

$$E_s - E_t = \frac{2(E(b) - E_u(T_1))}{1 + S_{ab}^2} \qquad (15)$$

(48) See for example: Kahn, O. *Molecular Magnetism*; Verlag Chemie: Weinheim, Germany, 1993; chapter 8.3 in particular.
(49) See ref 48, Figure 8.7 on p 164.
(50) (a) For the strong coupling, see for example: Bachler, V.; Chaudhuri, P.; Wieghardt, K. *Chem. Eur. J.* **2001**, *7*, 404 in particular eq 13. (b) For the weak coupling see ref 14a, in particular eq 34.
(51) See ref 50a, p 412.
(52) Amos, A. T.; Hall, G. G. *Proc. R. Soc. London* **1961**, *263A*, 483. King, H. F.; Stanton, R. E.; Kim, H.; Wyatt, R. E.; Parr, R. G. *J. Chem. Phys.* **1967**, *47*, 1936.
(53) We plotted the orbitals with the public domain program Molden.
(54) This is mentioned, for example, in ref 30, in particular p 90, section b.
(55) Ruiz, E.; Alemany, P.; Alvarez, S.; Cano, J. *J. Am. Chem. Soc.* **1997**, *119*, 1297.
(56) Caballol, R.; Castell, O.; Illas, F.; de P. R. Moreira, I.; Malrieu, J. P. *J. Phys. Chem.* **1997**, *101*, 7860−7866, in particular, p 7861 top.

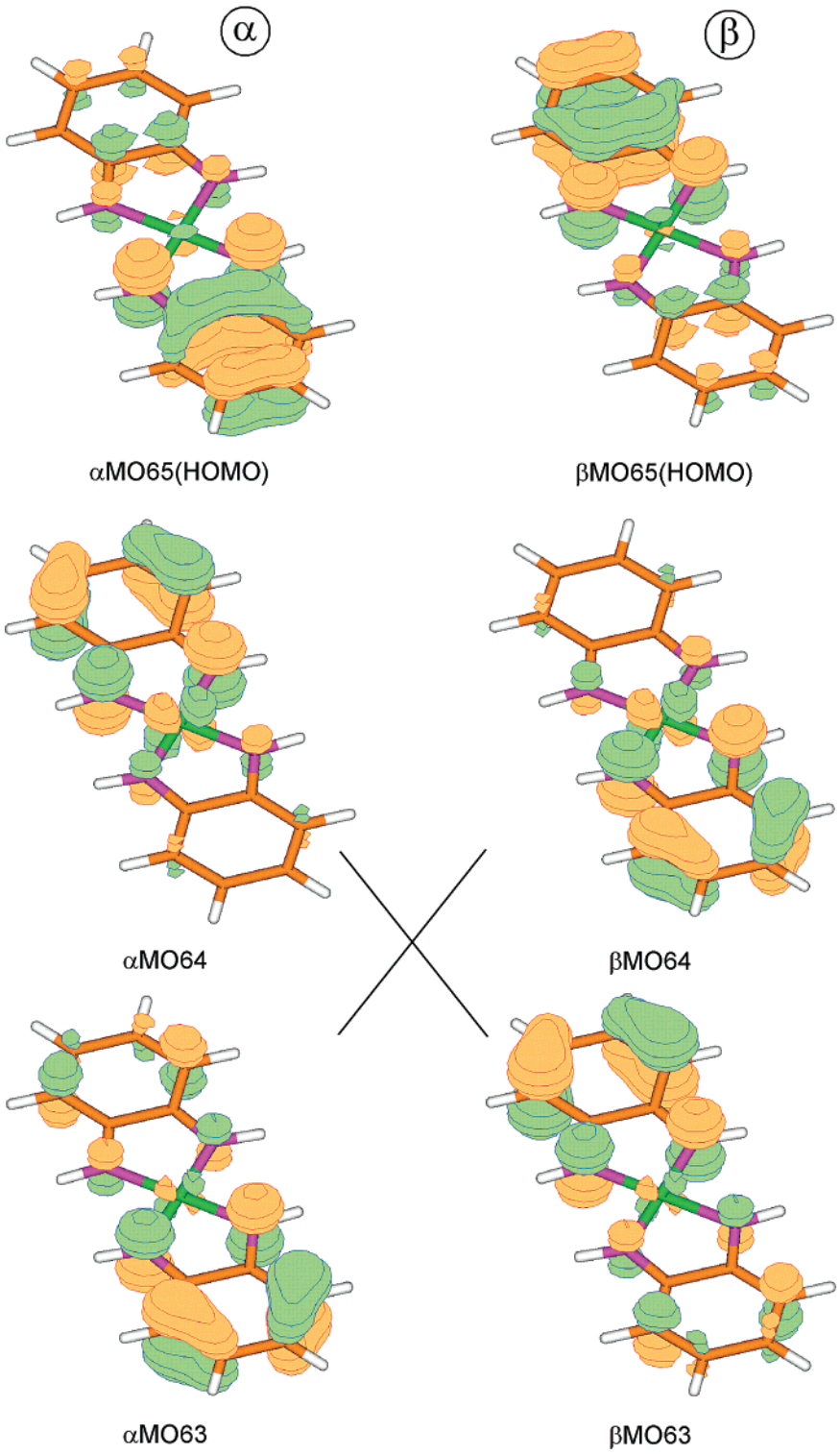

Figure 4. Qualitative scheme to single out the magnetic orbitals for nitrogen complex **1**. If the shapes of an α and a β MO match, their electrons are strongly antiferromagnetically coupled. The highest occupied α and β orbitals do not match in shape with any occupied orbital. They are the magnetic orbitals of **1**.

Thus, the singlet−triplet gap is also a function of the overlap integral S_{ab} of the magnetic orbitals a and b. However, eq 15 holds only when the spin polarization of the closed shells, induced by the weakly spin coupled electrons, can be neglected.[56] Instead of eq 15, we applied the even more general formula[14c,d,15a]

$$E_s - E_t = \frac{2(E(b) - E_u(T_1))}{2 - \langle \Psi(b)|S^2|\Psi(b)\rangle} \qquad (16)$$

where the spin polarization of the inner closed shells is reflected by the $\langle \Psi(b)|S^2|\Psi(b)\rangle$ value of the symmetry broken Kohn−Sham Slater determinant $\Psi(b)$. In the fol-

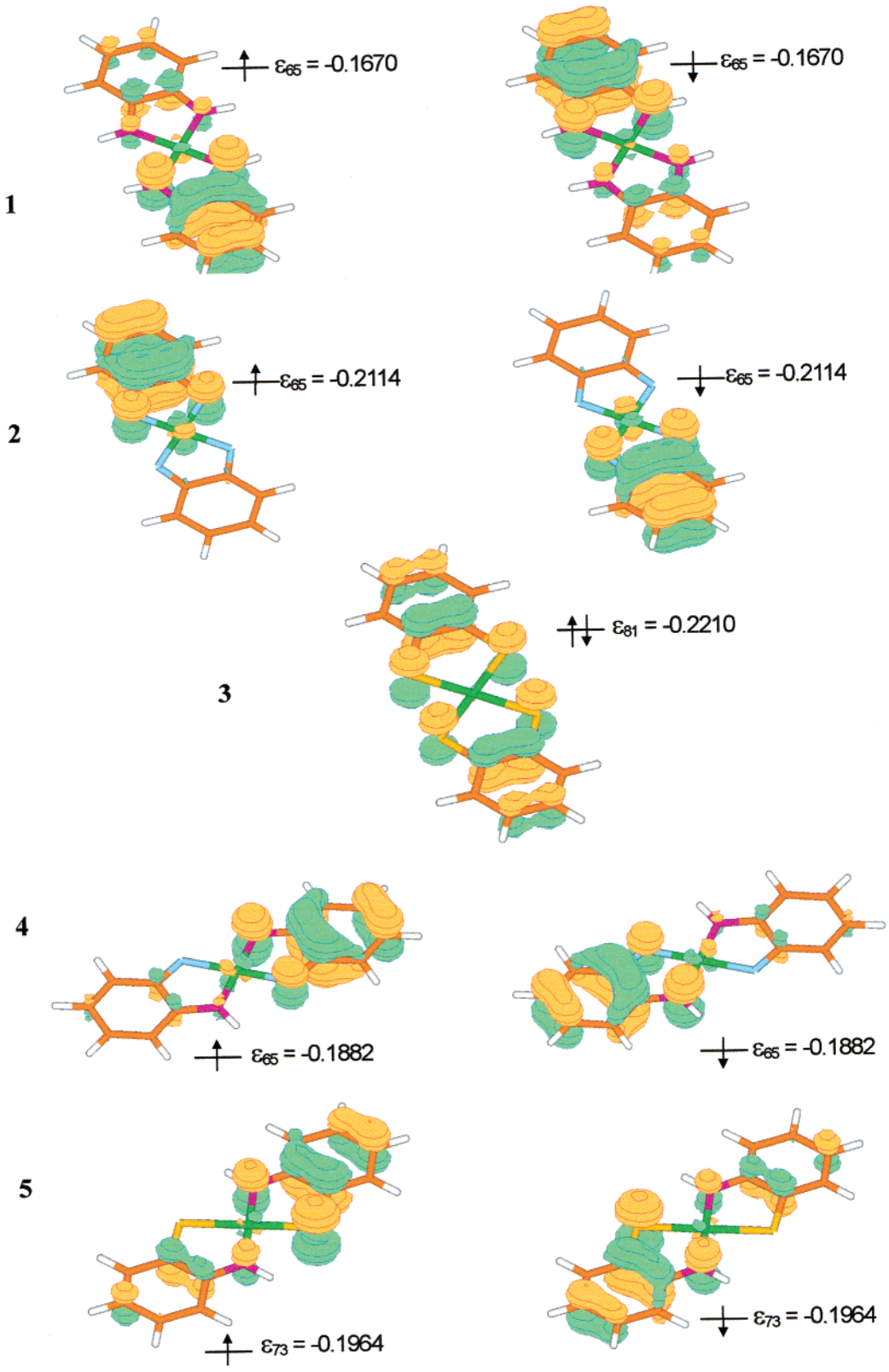

Figure 5. Magnetic orbitals of complexes **1**, **2**, **4**, and **5**. They are preferentially localized at one ligand but have tails at the other ligand. The larger the tails are in two magnetic orbitals, the larger the two electrons in the orbitals are antiferromagnetically coupled (see text). Sulfur complex **3** does not break symmetry spontaneously, and the HOMO is shown.

lowing, we apply eqs 14 and 16 to compute the singlet−triplet gaps for **1**, **2**, **4**, and **5**. Because of a cancellation of errors, eq 14 might yield more accurate gaps, but eq 16 is theoretically more profound. In the first row of Table 3, the total energies $E(b)$ are given. In the second and third rows, the energies for the high spin triplet $E_r(T_1)$ and $E_u(T_1)$ are recorded. They were computed within the restricted and unrestricted DFT procedure, respectively. $E_u(T_1)$ is almost

Table 3. Quantities for the Application of the Broken Symmetry Formalism[14a] to Compute the Singlet−Triplet Gaps in **1**−**5**[a]

quantity	N(**1**)	O(**2**)	S(**3**)	N, O(**4**)	N, S(**5**)
$E(b)$	−854.500814	−933.976855	−2225.88016 [$E(S_0)$]	−894.246629	−1540.198002
$E_r(T_1)$	−854.484753	−933.970367	−2225.856060	−894.235335	
$E_u(T_1)$	−854.486948	−933.972719	−2225.857778	−894.238155	−1540.182496
$\langle S^2\rangle_u$	2.0141	2.0134	2.0109	2.0205	2.0252
eq 14, cm^{-1}	−3043.2	−907.7	−4913.3	−1859.8	−3403.1
eq 16, cm^{-1}	−3613.1	−1537.2		−2711.1	−3870.5

[a] Total energies are given in atomic units. The smallest gap is computed for oxygen complex **2**. The diradical character should increase in the sequence **3** < **5** < **1** < **4** < **2** (see text).

Table 4. Energy Lowerings $E(S_0) - E(b)$ that Occur When the Space and Spin Symmetry of the Restricted DFT Solution Is Broken[a]

quantity	N(**1**)	O(**2**)	S(**3**)	N, O(**4**)	N, S(**5**)
$E(S_0)$	−854.500181	−933.968759	−2225.880165	−894.243032	−1540.197649
$E(b)$	−854.500814	−933.976855		−894.246629	−1540.198002
$E(S_0) - E(b)$	0.000633	0.008096		0.003600	0.000353
$\epsilon_i(S)$	−0.007334	−0.022044	0.005920	−0.010719	−0.005457
$\langle S^2\rangle$b	0.3155	0.8190		0.6280	0.2415

[a] Energies are given in atomic units. The largest lowering is calculated for the oxygen complex **2** that indicates the largest diradical character. This is also corroborated by the largest negative Eigenvalue ϵ_i of the stability matrix.

identical to $E_r(T_1)$ but, as expected,[57] always lower in energy than $E_r(T_1)$. This close agreement is substantiated by the total spin expectation values $\langle S^2\rangle_u$ that are near 2 (row 4). In row 5 of Table 3, singlet−triplet energy gaps computed from eq 14 are given. For oxygen complex **2**, the smallest value of 908 cm^{-1} is obtained, in qualitative agreement with the experimental gap value of 358 cm^{-1} determined for $[Cu^{II}(^{t-but}O_2')_2]$.[10] For all other complexes, larger gaps are computed. The rather large gaps are supported by the fact that these complexes are diamagnetic and the triplet states cannot be populated by increasing the temperature. In row 6 of Table 3, singlet−triplet gaps are recorded as obtained from eq 16. The applied $\langle\Psi(b)|S^2|\Psi(b)\rangle$ values are the numbers given in the last row of Table 4. As expected, the singlet−triplet gaps from eq 16 are larger than the gaps obtained from eq 14. Nevertheless, eqs 16 and 14 lead to singlet−triplet energy gaps that increase in the sequence **2** < **4** < **1** < **5**. For sulfur complex **3**, we can form the energy difference $E(S_0) - E_u(T_1)$ which yields a gap of 4913 cm^{-1}. If a large diradical character implies a small singlet−triplet gap,[54] the singlet diradical character of the complexes increases in the sequence **3** < **5** < **1** < **4** < **2**. This ordering is compatible with the capability of the ligands of **1**−**5** to stabilize the unpaired π electrons by delocalization over the phenyl rings. This delocalization is determined by the semiquinone character of the ligands which is related to the capability of the O, N, and S atoms to form double bonds with the phenyl rings. This double bond forming tendency increases in the sequence S < N < O.[58] This parallels the singlet diradical character as inferred from the computed singlet−triplet energy gaps. The weak double bond forming tendency of S atoms is in line with a large accumulation of spin density at the S atoms of **3** (Figure 3). Because of their proximity, however, the antiferromagnetic coupling is strong, and a small diradical character arises.

4.6. Shapes of Magnetic Orbitals. In this section, we show that the shapes of the magnetic orbitals (Figure 5) are qualitatively related to the singlet diradical character of the model complexes. The orbitals of **1** and **5** are localized at one ligand but have tails at the other one. This is not the case for **2**, and only very small tails are found for **4**. The tails of **1** and **5** permit the spin coupled electrons to approach each other more closely than in **2** and **4**. Consequently, the antiferromagnetic coupling in **1** and **5** should be larger than in **2** and **4**. Thus, the forms of the magnetic orbitals show that complexes **2** and **4**, with Ni−O bonds, should have a larger singlet diradical character than complexes **1** and **5** where Ni−N bonds are present. This is also substantiated by the energies of the KS magnetic orbitals which are displayed in Figure 5. From all model complexes, oxygen complex **2** has the magnetic orbitals of lowest energy. The magnetic orbital form combined with its low energy is compatible with a pronounced singlet diradical character of **2**. Only the highest doubly occupied KS orbital of sulfur complex **3** has a lower energy (Figure 5). This complex, however, does not break symmetry spontaneously.

4.7. Energy Lowering Induced by Symmetry Breaking. Another measure of the singlet diradical character is the energy lowering $E(S_0) - E(b)$ that results from a symmetry breaking of the restricted DFT solution. This energy lowering arises from the spin decoupling of electrons that have the tendency to localize in different parts of the molecule. We calculated an energy lowering of 0.4 and 5.1 kcal/mol for **1** and **2**, respectively (Table 4). An energy lowering of 2.3 and 0.2 kcal/mol are computed for **4** and **5**, respectively. Therefore, the singlet diradical character is found to increase in the sequence **5** < **1** < **4** < **2**. The same ordering of the

(57) The UHF wave function contains spin impurities from higher spin states that lower the energy below the RHF energy. See for example: Noodleman, L.; Case, D. A. *Adv. Inorg. Chem.* **1994**, *38*, 423 in particular, p 431. Noodleman, L.; Peng, C. Y.; Case, D. A.; Mouesca, J. M. *Coord. Chem. Rev.* **1995**, *144*, 199.

(58) The π bond energy increments for CO, CN, and SC are 90, 65, and 63 kcal/mol, respectively. See for example: Kutzelnigg, W. *Angew. Chem.* **1984**, *96*, 262 in particular, p 274, Table 2.

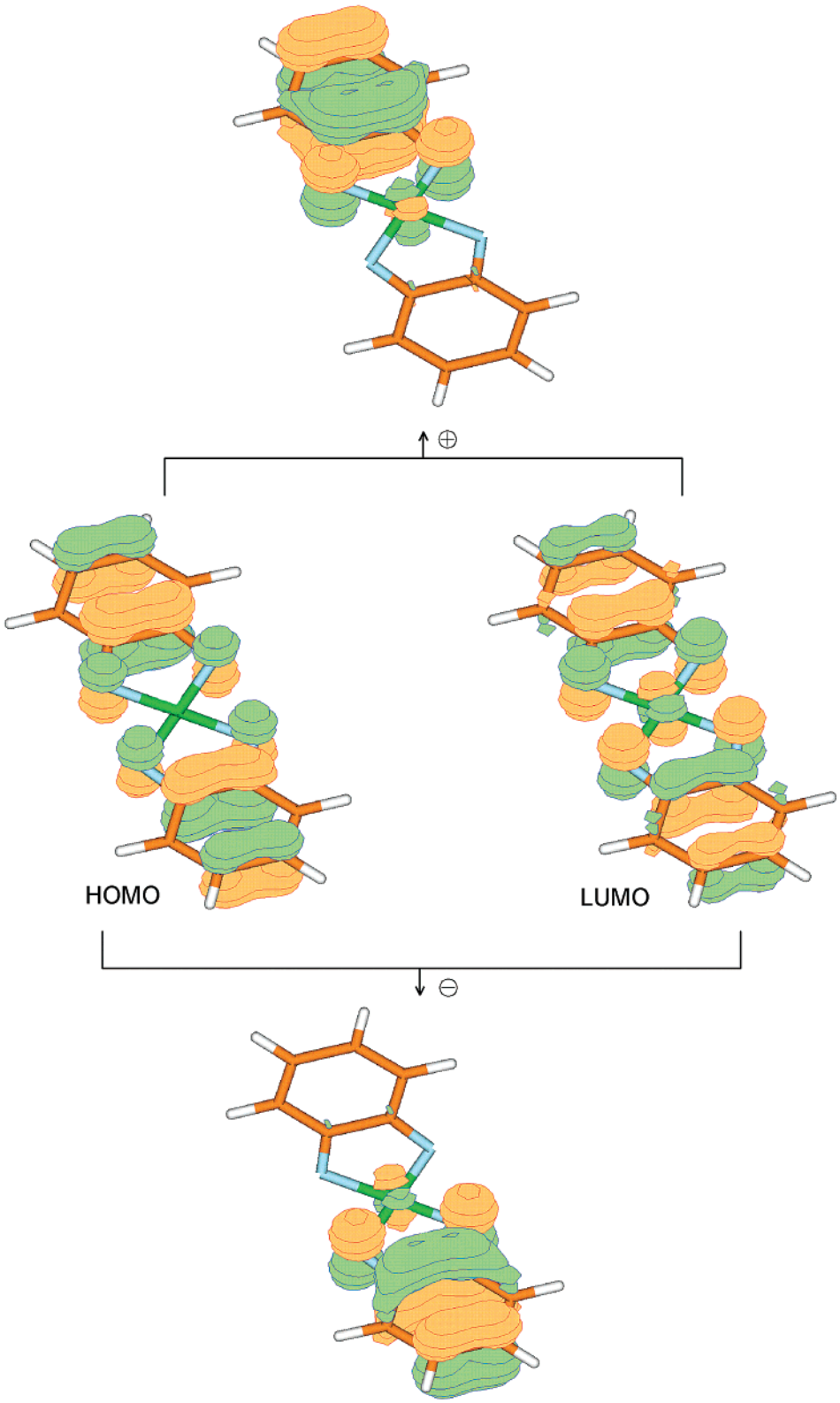

Figure 6. Two magnetic orbitals of oxygen complex **2** (above and below). They can be formed by the plus and minus linear combination of the HOMO and the LUMO of the restricted DFT solution.

singlet diradical characters is also supported by the only negative eigenvalues of the stability matrix[26] recorded in the fourth row of Table 4. A large negative eigenvalue implies the restricted solution has a strong tendency to become an unrestricted solution[59] which describes a diradical. A spontaneous symmetry breaking is absent in the sulfur complex **3**, and the lowest eigenvalue of the stability matrix is positive but rather small.

(59) See ref 26, eq 19 and subsequent comment.

Table 5. Diradical Characters n_{rad} of **1**−**5** as Computed by an Application of Equations 10 and 13[a]

complex	$\cos^2\theta$	n_{rad}(%) (eq 10)	n_{rad}(%) (eq 13)
S(**3**)			69.1
N, S(**5**)	0.9355	12.9	79.2
N(**1**)	0.9137	17.3	91.8
N, O(**4**)	0.8050	39.0	84.2
O(**2**)	0.7127	57.5	91.1

[a] Based on eqs 10 and 13, the diradical character increases in the sequence **5** < **1** < **4** < **2** and **3** < **5** < **4** < **2** < **1**, respectively.

4.8. Spin Expectation Value. The expectation values of the total spin operator S^2 are recorded in row 5 of Table 4. They were computed by forming the expectation value with a Slater determinant made up by the occupied KS orbitals. The S^2 expectation value is a typical two-electron property. It should be computed by means of the two-electron density function as pointed out by Wang et al.[60] However, the use of a simple Slater determinant often produces reasonable spin expectation values.[61] The symmetry broken wave functions for **1**, **2**, **4**, and **5** are primarily a linear combination of spin pure singlet and triplet wave functions. If the singlet−triplet energy gap in a singlet diradical is small, the symmetry broken wave function contains singlet and triplet wave functions with similar weights. Therefore, a spin expectation value near 1.0 is expected for a pronounced singlet diradical. This condition holds best for complex **2** for which we compute a spin expectation value of 0.8190. Therefore, oxygen complex **2** has the smallest singlet−triplet energy gap and the largest singlet diradical character.

5. Diradical Character of the Target Complexes

To quantify the diradical character by means of eq 10 (Section 3), we have to assume that the diradical properties are solely determined by the two electrons in the magnetic orbitals of the symmetry broken DFT solutions. Moreover, the two magnetic orbitals should be reasonably approximated by the plus and minus linear combination of two frontier KS orbitals of the restricted DFT solution. We realize that this condition holds for oxygen complex **2** (Figure 6), but it is valid also for **1**, **4**, and **5** (not shown). Therefore, the application of the transformation (eq 3) is legitimate, and $\cos^2\theta$ and n_{rad} can be computed by means of eqs 6 and 10, respectively. We applied for this purpose the S^2 expectation values as obtained from the symmetry broken B3LYP DFT solution. The results are summarized in Table 5. The largest diradical character of 57.5% is computed for oxygen complex **2.** Again, the diradical character appears with the same ordering as determined in the previous sections, that is, **5** < **1** < **4** < **2**.

6. Comparison of ab Initio CASSCF and DFT Results

In Section 4.5, the broken symmetry DFT formalism[14,16] has been applied to compute the singlet−triplet gaps for model complexes **1**−**5**. Here, we pursue the idea that small singlet−triplet gaps are solely determined by the energy needed to excite one electron out of the HOMO. This notion suggests the use of the complete active space self-consistent field (CASSCF) procedure to correlate explicitly only the two π electrons of the HOMOs. We applied the CASSCF-(2,8) scheme where two electrons are distributed among an active space of 8 MOs. We used the unrestricted natural orbital (UNO) CASSCF approach to define the active space.[62] At first, RHF solutions for complexes **1**−**5** were obtained. Subsequently, the symmetry broken UHF wave functions and the UNOs were obtained by diagonalizing the one-electron density matrix *of the symmetry broken state*.[62] We obtained the UNOs in a sequence of decreasing occupation numbers. For all model complexes, we could distinguish two ordered groups of UNOs. One group is characterized by occupation numbers close to 2. The other group comprises UNOs with occupation numbers close to 1 and smaller. We used the first eight members of the last group of UNOs as active space start orbitals for the CASSCF(2,8) computations. The orbital shapes of the first two members of the CAS were found to be almost identical to the HOMO and LUMO forms depicted in Figure 6. Thus, the LUMOs have a small but nonnegligible d character at the Ni atom. Therefore, exchange pathways that imply an electron transfer from the ligands to the central Ni atom are accounted for in the CASSCF(2,8) computations. Our computational results are compiled in Table 6. For all complexes, the singlet ground state is lower in energy than the triplet state. This accords with the experimental finding that all complexes are diamagnetic. This agreement is further support for the known fact[63] that the active electron approach, even when applied at the CASSCF(2,2) level, predicts correctly the ground-state spin multiplicity. In the third row of Table 6, the computed singlet−triplet gaps are given. In the symmetry broken DFT formalism, we can assume that error cancellation in eq 14 produces singlet−triplet gaps of reasonable accuracy (Table 3).[16] Consequently, the CASSCF-(2,8) gaps are much too small. This finding accords with the results of Staemmler and co-workers who observed that at the CASSCF level of theory the exchange coupling constants J are too small.[64] The inclusion of dynamic correlation into the computations is mandatory to obtain accurate coupling constants.[64] The singlet−triplet gaps in Table 6 indicate an increase of the diradical character again as **3** < **5** < **4**< **2** < **1**.

As outlined in Section 3, the magnitude of the configuration interaction coefficient c_d of the first doubly excited configuration is also an indicator for the singlet diradical character. A large covalent character of the two-electron wave function for the weakly spin coupled electrons implies an absolute c_d value near $1/\sqrt{2}$. We used the c_d values (Table 6) to compute the singlet radical index n_{rad} by means of eq 13, and the values are displayed in column 4 of Table 5. We observe that the n_{rad} values from eq 13 are much larger

(60) Wang, J. H.; Becke, A. D.; Smith, V. H. *J. Chem. Phys.* **1995**, 102, 3477.
(61) See for example ref 60, in particular the columns of Table 1 labelled "Noninteracting" and "Exact". See also ref 18, in particular p 1755.
(62) Bofill, J. M.; Pulay, P. *J. Chem. Phys.* **1989**, *90*, 3637. Pulay, P. J.; Hamilton, T. P. J. *Chem. Phys.* **1988**, *88*, 4926.
(63) Illas, F.; de P. R. Moreira, I.; de Graaf, C.; Barone, V. *Theor. Chem. Acc.* **2000**, *104*, 265 in particular, p 268 below.
(64) Wang, C.; Fink, K.; Staemmler, V. *Chem. Phys.* **1995**, *192*, 25; *Chem. Phys.* **1995**, *201*, 87.

Table 6. Singlet−Triplet Gaps $E(S_0) - E(T_1)$ as Computed with the CASSCF(2, 8) Procedure[a]

quantity	N(**1**)	O(**2**)	S(**3**)	N, O(**4**)	N, S(**5**)
$E(S_o)$	−848.854854	−928.427313	−2218.989826	−888.752782	−1533.870667
$E(T_1)$	−848.854288	−928.426204	−2218.979933	−888.749446	−1533.866044
$E(S_0) - E(T_1)$ cm^{-1}	−124.2	−243.4	−2171.2	−738.7	−1014.6
c_d	−0.649089	−0.644302	−0.488697	−0.595272	−0.559778

[a] Total energies are given in atomic units. The smallest gap is derived for oxygen complex **2**. The diradical character is found to increase in the sequence **3** < **5** < **4** < **2** < **1.**

than the corresponding values obtained with eq 10 (Table 5), and they indicate a singlet diradical character that increases as **3** < **5** < **4** < **2** < **1**. This is almost the same ordering as that derived from the symmetry broken DFT solutions. The only exception is nitrogen complex **1** that should have a slightly larger diradical character than oxygen complex **2**.

7. Discussion and Conclusion

In this work, we applied several criteria to evaluate the singlet diradical character of model complexes **1**−**5** shown in Scheme 1. One criterion was the energy lowering of the symmetry broken DFT solution when compared to the restricted DFT solution. A large energy lowering indicates a large diradical character. Another criterion is the singlet−triplet energy gap. If the gap is small, only a small amount of energy is needed to invert one spin, and the molecule should have a large diradical character. A further criterion was based on the form of the magnetic orbitals. If the space parts of the α and β magnetic orbitals are not overlapping, their two electrons of opposite spins avoid each other. This is characteristic for a large singlet diradical character. Alternatively, a large overlap of the magnetic orbitals implies a strong radical−radical interaction and a weak diradical character. In the broken symmetry formalism, this overlap is determined by the variational principle, and the minimal energy is linked to a definite overlap. In the restricted CI formalism, the diradical character is described by mixing in a doubly excited singlet configuration to the closed shell Slater determinant. In the symmetry broken approach, however, a singly excited triplet wave function is additionally introduced into a nominal singlet state. The triplet state also corresponds to a state with "separated electrons". Thus, the ionic versus covalent character determined by the variational principle is similar in the restricted CI and the broken symmetry approaches. We mention here that the broken symmetry state does not represent an equal mixture of a singlet and a triplet state as is often assumed. This holds only in the limit of vanishing intersite interaction where the singlet and the triplet state are degenerate. In the strong interaction limit, the broken symmetry state has the variational freedom to become a closed shell singlet state that is a pure spin state.

Most of our diradical character criteria are based on the premise that a symmetry broken DFT solution exists for a molecule. An exact DFT solution, however, would produce the exact N-representable density that corresponds uniquely to an electronic wave function.[65] Such a wave function transforms as an irreducible representation of the molecular point group, and it describes a pure spin state. Thus, Cremer and co-workers state in their theoretical paper on the Bergman reaction: "In Kohn−Sham calculations with approximate functionals, symmetry breaking in the Kohn−Sham ground state simply reflects the shortcomings of the approximate functionals used".[66] Singlet diradicals have an inherent multireference character, and static correlation effects are important. It is the approximate and symmetry broken DFT solution that simulates the static correlation effects. Such a symmetry broken DFT solution occurs when the closed shell DFT solution is unstable. Such instabilities have been investigated by Bauernschmitt and Ahlrichs.[67] One of their results is an ordering of the common exchange correlation functionals with respect to the stability of their restricted DFT solutions. If the exact exchange correlation functional would be available, the restricted solution would be symmetry adapted and stable. However, even in the exact DFT solution for a singlet diradical, electron correlation would keep two electrons of opposite spin far apart,[68] but the symmetry breaking would vanish. Thus, the symmetry breaking of a restricted approximate DFT solution should be considered as a first indicator for the presence of a singlet diradical. This reasoning highlights the importance of the recent work of Staroverov and Davidson who identify a singlet diradical character by means of newly defined densities of effectively unpaired electrons.[69] This procedure has been applied by Budzelaar et al. who discussed the diradical characters of MnL_2^+ and FeL_2^{2+} complexes.[70]

The symmetry broken B3LYP solutions showed that complex **2** has the largest singlet diradical character. The restricted BLYP solutions for **1**−**5**, however, turned out to be stable. This finding accords with the results of Bauernschmitt and Ahlrichs who found that the Hartree−Fock exchange component of the hybrid exchange functional leads to a significant instability of the restricted DFT solution.[67] This is also corroborated by the work of Cremer and co-workers who showed that the instability of the DFT solution

(65) Parr, R. G.; Yang, W. *Density-Functional Theory of Atoms and Molecules*; Oxford University Press: New York, 1989; section 3.3, p 53.
(66) See ref 18, in particular, p 1755.
(67) Bauernschmitt, R.; Ahlrichs, R. *J. Chem. Phys.* **1996**, *104*, 9047.
(68) This is analogous to the H_2 dissociation problem. The exact DFT solution and wave function must describe the correct decoupling of the electron spins that leads to two hydrogen atoms. For a discussion of the dissociation behaviour of the restricted and unrestricted DFT solutions for H_2, see for example, ref 17, in particular Figure 4.
(69) Staroverov, V. N.; Davidson, E. R. *Int J. Quantum Chem.* **2000**, *77*, 316. Staroverov, V. N.; Davidson, E. R. *Int. J. Quantum Chem.* **2000**, *77*, 651. Staroverov, V. N.; Davidson, E. R. *J. Am. Chem. Soc.* **2000**, *122*, 186.
(70) Budzelaar, P. H. M.; de Bruin, B.; Gal, A. W.; Wieghardt, K.; van Lenthe, J. H. *Inorg. Chem.* **2001**, *40*, 4649−4655.

for a singlet diradical is linked to the presence of Hartree−Fock exchange in the DFT exchange potential.[71] Thus, our results may depend on the degree of Hartree−Fock exchange. However, the B3LYP procedure leads to reasonable exchange coupling constants for transition metal complexes.[55] Therefore, at least the relative ordering of diradical characters should be correct. The obtained sequence **3** < **5** < **1** < **4** < **2** can be qualitatively understood from the stability of the semiquinone forms of the ligands. This stability depends on the ability of the coordinating atoms to form partial double bonds with the ring carbons. This ability increases in the series S < N < O[58] and provides a satisfactory rationale for the observed trends in the structure and the singlet diradical character of the complexes studied in this work.

(71) See ref 18, p 1752.

IC0113101